CMLS, Cell. Mol. Life Sci. 62 (2005) 1400–1408
1420-682X/05/121400-09
DOI 10.1007/s00018-005-5094-3

CMLS Cellular and Molecular Life Sciences

Research Article

A relevant in vitro rat model for the evaluation of blood-brain barrier translocation of nanoparticles

E. Garcia-Garcia [a], S. Gil [b], K. Andrieux [a, *], D. Desmaële [c], V. Nicolas [d], F. Taran [e], D. Georgin [e], J. P. Andreux [b], F. Roux [f] and P. Couvreur [a]

[a] Laboratory of Pharmaceutical Technology and Biopharmacy, UMR CNRS 8612, Faculty of Pharmacy, University of Paris-XI, 92296 Châtenay-Malabry (France), Fax +33 146 61 93 34, e-mail: karine.andrieux@cep.u-psud.fr
[b] UPRES 2706, Faculty of Pharmacy, University of Paris-XI, 92296 Châtenay-Malabry (France)
[c] Department of Organic Chemistry, Faculty of Pharmacy, University of Paris-XI, 92296 Châtenay-Malabry (France)
[d] Unit of Imagery IFR 75, Faculty of Pharmacy, University of Paris-XI, 92296 Châtenay-Malabry (France)
[e] Department of Radiolabeled Molecules, CEA/Saclay bat, 547, 91191 Gif sur Yvette (France)
[f] Unit of Neuro-Pharmaco-Nutrition INSERM U.26, hôpital Fernard Widal, 75010 Paris (France)

Received 4 March 2005; accepted 14 April 2005
Available online 18 May 2005

Abstract. Poly(MePEG$_{2000}$cyanoacrylate-co-hexadecylcyanoacrylate) (PEG-PHDCA) nanoparticles have demonstrated their capacity to reach the rat central nervous system after intravenous injection. For insight into the transport of colloidal systems across the blood-brain barrier (BBB), we developed a relevant in vitro rat BBB model consisting of a coculture of rat brain endothelial cells (RBECs) and rat astrocytes. The RBECs used in our model displayed and retained structural characteristics of brain endothelial cells, such as expression of P-glycoprotein, occludin and ZO-1, and immunofluorescence studies showed the specific localization of occludin and ZO1. The high values of transendothelial electrical resistance and low permeability coefficients of marker molecules demonstrated the functionality of this model. The comparative passage of polyhexadecylcyanoacrylate and PEG-PHDCA nanoparticles through this model was investigated, showing a higher passage of PEGylated nanoparticles, presumably by endocytosis. This result was confirmed by confocal microscopy. Thanks to a good in vitro/in vivo correlation, this rat BBB model will help in understanding the mechanisms of nanoparticle translocation and in designing new types of colloidal carriers as brain delivery systems.

Key words. Rat blood-brain barrier in vitro model; brain endothelial cell; tight junction; PEGylated-nanoparticle; transport of nanoparticle.

Drug delivery to the brain is a challenge, because this tissue benefits from very efficient protection. The same mechanisms that protect the brain from foreign substances also restrict the entry of many potentially therapeutic agents. Thus, numerous new chemical entities for treating brain disorders are not clinically useful due to the presence of the blood-brain barrier (BBB). To increase the bioavailability of these molecules, nanoparticles can now be used to deliver them to the brain [1]. In general, drugs can be dissolved, entrapped, encapsulated or attached to a nanoparticle matrix, serving as 'trojan horses' for a wide variety of new chemical entities. In such a manner, drug loading onto nanoparticles has been found by many authors [2–4] to modify the cell and tissue distribution. This may lead to a more selective delivery of biologically active compounds to improve drug efficacy and reduce the drug toxicity. In this context, Kreuter's group has developed poly(butylcyanoacrylate) (PBCA) nanoparticles onto the

* Corresponding author.

surface of which the desired drug was adsorbed and then overcoated with polysorbate 80 (PS-80). These nanoparticles have been used as a vector for the brain delivery of dalargin [5], loperamide [6] and doxorubicin [7]. However, recently, Olivier et al. [8] suggested that the PBCA nanoparticles coated with PS-80 displayed some toxic effect towards the BBB by opening the tight junctions between endothelial cells in the brain microvasculature, thus creating a paracellular pathway for nanoparticle translocation. This toxicity, which was not observed in either the in vitro or in vivo studies performed by Kreuter et al. [9], could be due to the desorption processes of PS-80. This process, in addition to the drug desorption, could explain the efficacy loss of dalargin adsorbed onto PS-80 nanoparticles 5 min after intravenous (IV) injection [10]. One emerging strategy to avoid the desorption process is the formation of nanoparticles from an amphiphilic copolymer in which the hydrophobic block itself is able to form a solid phase where hydrophobic drugs can be encapsulated, while the hydrophilic block remains as a surface-exposed cloud (core-shell nanoparticles). In fact, when decorated with hydrophilic polymers such as polyethylene glycol (PEG), nanoparticles are protected by a steric barrier against interactions with plasma proteins, resulting in a longer circulation time in the blood compartment [11, 12]. This prolongation of the half-life in plasma will increase the chances of nanoparticles reaching the central nervous system (CNS) where the biodegradation of the nanoparticles would allow a prolonged leakage of the drug. More surprisingly, in vivo studies have also shown that poly($MePEG_{2000}$cyanoacrylate-co-hexadecylcyanoacrylate (PEG-PHDCA) nanoparticles which have a shorter plasma half-life than other long-circulating carriers were also able to penetrate the CNS of normal rats when the BBB was intact, to a significantly higher degree than the other systems [13]. These results have suggested that the mechanism of nanoparticle translocation through the BBB is influenced by interactions between brain endothelial cells and nanoparticles with a specific surface composition. From this perspective, the development of a relevant rat BBB model was of primary importance for understanding the mechanism underlying nanoparticle translocation.

Many protocols have been reported for the culture of brain endothelial cells. These techniques generally employ large animals, such as bovine or porcine species which offer obvious advantages in terms of starting material [14–17]. However, since in vivo experimental models of CNS diseases are generally effected in the rat, in vitro models of the BBB with bovine endothelial cells may be inappropriate for investigating the mechanism of nanoparticle translocation, especially when blood protein adsorption and opsonization may be involved. Rodent brain endothelial cells in culture present rapid dedifferentiation and a loss of their specific characteristics [18]. Some in vitro cultures of rat endothelial cells have been developed [19, 20], but no model is well established. Therefore, investigation of nanoparticle translocation required the development of a relevant and well characterized rat model of the BBB where the most important in vivo characteristics of the BBB such as tight junction (TJ) localization, P-glycoprotein (P-gp) expression and permeability coefficient (Pe) could be investigated. The purpose of this study was to establish an in vitro rat model of the BBB based on a coculture, to evaluate colloidal-drug-carrier translocation.

Materials and methods

Cell isolation and culture

All protocols involving animals comply with European Community guidelines for the care and use of laboratory animals (Directive n°. 86/609 CEE).

Rat brain capillaries

These were isolated using the procedure of Szabo et al. [19] modified as described. Brain cortex from 2-week-old Sprague-Dawley rats (Charles River Laboratories, L'Arbresle, France) was used after elimination of meninges and grey matter. Tissues were digested at 37 °C in collagenase-dispase solution for 1 h 30 min (Boehringer, Mannheim, Germany). Cold DMEM-F12 (Invitrogen, Cergy Pontoise, France) was added to the homogenate and centrifuged at 1000 g, 4 °C for 5 min. The pellet was resuspended in 25% Bovine serum albumin (BSA) (Sigma-Aldrich, St. Louis, Mo.) and centrifuged at 1500 g, 4 °C for 15 min. The resulting pellet was then digested at 37 °C for 1 h in enzymatic solution as above. This new digest was filtered through a 10-µm-pore-size nylon mesh and washed three times with DMEM-F12. Finally, the nylon mesh was recovered and the capillary fragments were washed off the mesh by propulsion of culture medium EBM-2 containing 10% fetal bovine serum (FBS), antibiotic cocktail (Cambrex, Verviers, Belgium) and 3 µg/ml puromycin (Sigma-Aldrich). Briefly, this treatment with 3 µg/ml puromycin for 3 days after brain capillary isolation eradicates almost all the contaminating cells because puromycin is cytotoxic for cells lacking P-gp. Rat brain endothelial cells (RBECs) express a high level of P-gp which prevents intracellular accumulation of puromycin and cytotoxicity. Puromycin allows the proliferation of only RBECs (98–99% purity) with the characteristic shape and a high level of transendothelial electrical resistance of the monolayer formed [18]. The capillary fragments were seeded on collagen S (Boehringer) coated plastic dishes 60 mm in diameter (Corning Costar, Cambridge, Mass.) and incubated in a water-saturated atmosphere of air and 5% CO_2 at 37 °C. After 3 days, culture medium was replaced, puromycin

was removed from the culture medium and EBM-2 MV singlequots (Cambrex) were added. To confirm the purity of RBECs, the expression of a specific endothelial cell marker (von Willebrand factor) was identified. Five-day-old cultures were fixed at room temperature in PBS containing 1% paraformaldehyde (20 min) and incubated with the rabbit polyclonal anti-human von Willebrand factor antibody (DAKO; 1:50 dilution, 10 min). Cells were then stained according to the protocol of the DAKO (Trappes, France) LSAB2 Kit, Peroxidase for use on rat specimens (Universal K609).

Astrocytes

These cells were isolated from brain cortex of Sprague-Dawley rats 1–3 days after birth. After elimination of meninges, the cortex was disaggregated through a 10-ml pipette in 4×10^{-3}mol/-EDTA (Invitrogen*)* in Ca^{2+}/Mg^{2+} free PBS for 10 min at room temperature. The homogenized tissue was filtered through an 80-µm filter. The remaining cells were directly plated on 75-cm^2 culture flasks in DMEM/F12 medium containing 20% FBS and antibiotics (penicillin 100 U/ml, streptomycin 100 µg/ml). The medium was changed every 3 days. After 7 days, the flasks were shaken at 37 °C for 24 h in order to eliminate the contaminating microglia. Subsequently, the astrocytes were transferred at first passage to the bottom of the 12-well plates at a concentration of 50,000cells/cm^2 to form the in vitro model. As with RBECs, the expression of a relatively specific astrocyte cell marker (glial fibrillary acidic protein, GFAP) was determined according to the same protocol.

Characterization of the in vitro BBB model

RBECs at first passage were cultured on type-IV-collagen-coated Transwells (3.0 µm pore size, 1 cm^2 growth area; Corning Costar) at a density of 100,000 cells/cm^2. The Transwells were placed into 12-well plates containing astrocytes cultures. The coculture medium was EBM-2 MV, supplemented with 5% (v/v) FBS and singlequots.

Immunofluorescence

RBECs and human umbilical vascular endothelial cells (HUVECs) were fixed in PBS containing 1% paraformaldehyde (20 min) and then permeabilized (15 min with 0.1% Triton X-100 in PBS). Cells were exposed to 1% FBS for 30 min to block non-specific binding sites. Polyclonal rabbit anti- ZO-1 or anti-occludin (Zymed, San Francisco, Calif.) was applied overnight in a humidified atmosphere and the cells were then washed three times with PBS. The secondary antibody [FITC-conjugated goat anti-rabbit IgG (Zymed)] was applied for 1 h, after which cells were washed five times. Rhodamine-conjugated phalloidin (Sigma-Aldrich) was applied for 15 min, followed by three washes with PBS. Three different controls were performed for each labeling experiment: (i) specific antibody controls, (ii) incubation with only the secondary-labeled antibodies, and (iii) estimation of autofluorescence of unlabeled cells.

Stained specimens were viewed with an LSM 510 Zeiss confocal inverted microscope equipped with a Zeiss ×63/1.4 NA oil immersion objective lens. Fluorescence images were acquired with argon (wavelength 488 nm) and helium neon (wavelength 543 nm) lasers.

Western blot analysis

Western blot was used to determine P-gp, occludin and ZO-1 expression. Briefly, cells were scraped from the bottom of the filter insert and solubilized with lysis buffer (10 mM Tris pH 7.5, 5 mM EDTA, 125 mM NaCl, 1% Triton, 0.1% SDS and protease inhibitor cocktail; Sigma-Aldrich). The protein concentration was determined using the colorimetric Bicinchoninic Assay Kit (Uptima, Interchim, Montlucon, France) with BSA as standard. Five micrograms of cellular proteins was subjected to SDS-polyacrylamide gel electrophoresis with 8% polyacrylamide and transferred onto a nitrocellulose membrane which was then incubated with primary antibody [C219 (DAKO), anti-ZO-1, anti-occludin, diluted 1:100], followed by a peroxidase-conjugated anti-rabbit IgG as secondary antibody (DAKO). The immunoreactive bands were visualized with an enhanced chemiluminescent system (Amersham Biosciences, Saday, France).

Transendothelial electrical resistance

Transendothelial electrical resistance (TEER) of RBEC monolayers in the presence or absence of astrocytes was measured with an ENDOHM tissue resistance measurement chamber (World Precision Instruments, Sarasota, Fla.). The average of values corresponding to five coated Transwells (without cells) was subtracted from the resistance of transwells with RBECs to give the resistance of the cell monolayer. The results were expressed in Ωcm^2.

Permeability studies

Cell layer permeability was determined concurrently with the serial measurements of TEER. The paracellular permeability across RBEC monolayers was measured using [^{14}C]sucrose (0.5 µCi/ml) and [^{3}H]inulin (1 µCi/ml; Amersham) as hydrophilic markers. Permeability studies were undertaken at 37 °C in permeation medium (EGM-2 MV medium with 5% FBS). At selected times points of 20, 40, 60, 120, 180 and 240 min after the addition of the sucrose/inulin solution in the upper compartment, the inserts were subsequently transferred to other wells to minimize back diffusion of compound to the upper compartment. At the end of the experiments, for each time point, aliquots were taken from the lower compartments, and radioactivity was determined (BECKMAN model LS 6000TA). Permeabilities of RBECs were calculated

according to the method of Siflinger-Birnboim et al. [21] using the clearance principle as described previously [22]. All experiments were repeated at least ten times.

Biodegradable cyanoacrylate nanoparticle preparation and characterization

[^{14}C]radiolabeled nanoparticles were prepared with either poly(hexadecylcyanoacrylate) ([^{14}C](PHDCA) or [^{14}C] PEG-PHDCA. These polymers were prepared at the Commissariat à l'Energie Atomique (Saclay, France) according to previously described protocols [11, 23]. [^{14}C]PHDCA and [^{14}C]PEG-PHDCA had a specific activity of 5.8 and 1.5 µCi/mg, respectively. Biodegradable [^{14}C]PHDCA and [^{14}C]PEG-PHDCA nanoparticles were obtained and characterized by the methods previously described [24]. Nanoparticle degradation products were also obtained as previously described [25]. Fluorescent nanoparticles were prepared with the same method except that non-radiolabeled polymers were used and nile red (Interchim, Montluçon, France), a fluorescent marker (25 µg), was added.

Translocation of nanoparticles and [^{14}C]PEG-PHDCA nanoparticle degradation products across the in vitro BBB model

Experiments were initially conducted to determine the ability of nanoparticles to cross the RBEC monolayer. This was accomplished at 37 °C at a concentration of 20 µg/ml of boths nanoparticle types between 13 and 17 days in coculture and monoculture. Translocation experiments were conducted from the upper to lower compartments with sampling time points of 20, 40, 60, 120, 180 and 240 min, and [^{3}H]inulin was used to verify in vitro BBB model integrity. Free transport of nanoparticles through the coated Transwell lacking RBECs was checked. For each time point, aliquots were taken from the lower compartments, and radioactivity was determined. Studies were also undertaken with degraded [^{14}C]PEG-PHDCA nanoparticles.

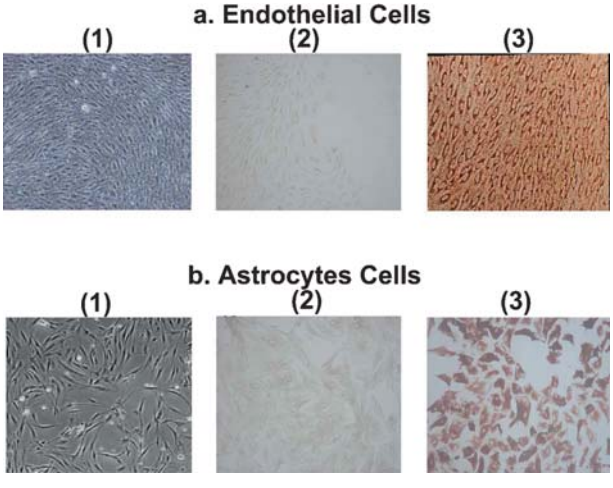

Figure 1. Characteristics of cultured rat brain endothelial cells (*a*) and astrocytes (*b*) by phase-contrast microscopy and immunocytochemistry labeling: (1) unlabeled cells, (2) labeled cells with no specific primary antibodies, (3) labeled cells with specific primary antibodies–von Willebrand factor in cultured RBECs (*a*3) and GFAP in astrocytes (*b*3).

RBEC uptake of nanoparticles

To determine nanoparticle uptake, RBECs were then incubated with a suspension of fluorescent nanoparticles (20 µg/ml) in permeation medium for 1 h at 37 °C. At the end of incubation, the cell monolayers were rinsed three times with PBS to remove excess nanoparticles. Cell monolayers were then fixed with paraformaldehyde (1%) in PBS for 15 min and samples were analyzed with a confocal microscope.

Statistical analysis

All data are expressed as means (n=6) ± SE. Sets of data were compared using the non-parametric Mann-Whitney test. Differences were considered significant at $p<0.05$. The reproducibility of our model was statistically analyzed with ten independent cocultures using the TEER values (n = 5) and the permeability coefficients for sucrose and inulin (n = 5).

Results

Assessment of the rat BBB model

We succeeded in routinely obtaining RBEC cultures with 98% purity as demonstrated by granular cytoplasmic staining for von Willebrand Factor, a specific marker of endothelial cells (fig. 1a). The purity of astrocyte cultures, which do not form a monolayer, was also checked by labeling cells with GFAP antibody (fig. 1b). Because this marker is not specific for astrocytes but is also present in glial cells, the identification of astrocytes was confirmed by morphology observation (fig. 1b) as in previous studies [18].

The in vitro BBB model was realized in a Transwell system using RBECs on one side of a polyester filter and rat astrocytes in the bottom well. It was characterized by analysis of the expression and localization of proteins which are specific to brain endothelial cells and by measurements of transendothelial electrical resistance and permeability to small molecules.

The expression in RBECs of specific proteins, like P-gp and two proteins incorporated into TJs, occludin and ZO-1, was detected by immunoblotting studies. Western blots revealed the presence of theses proteins: P-gp was detected as a specific band of 170 kDa, occludin as a band migrating at 60 kDa, and ZO-1 protein at 225 kDa (fig 2a).

The localization of the transmembrane protein, occludin, and of the cytoplasmic protein, ZO-1, in RBECs in cocul-

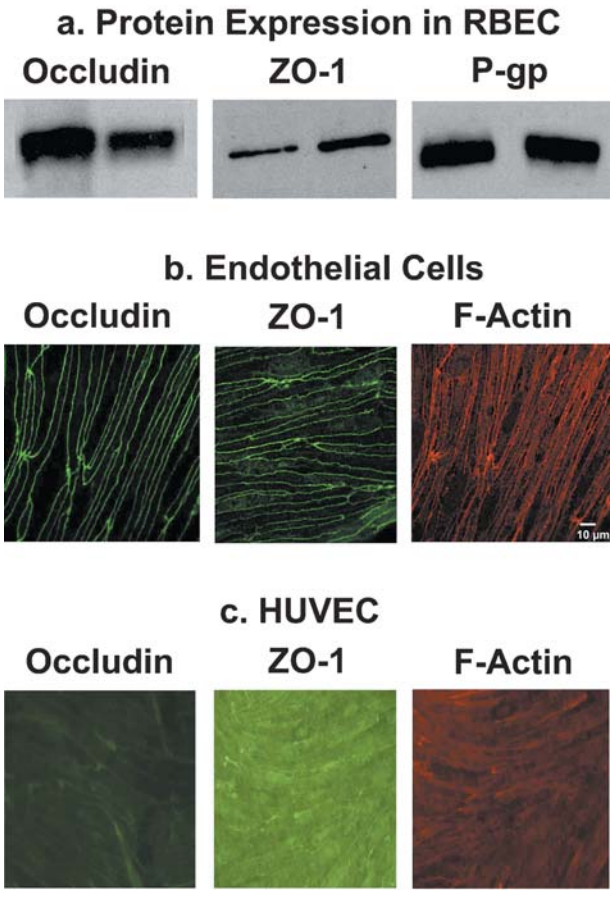

Figure 2. *a* Western blot analysis of occludin, ZO-1 and P-gp in RBECs after 13 days in a coculture system. (*b*, *c*) Confocal microscopy of the distribution of occludin, ZO-1 and F-actin in RBECs (*b*) and HUVEC (*c*) after 13 days in coculture. F-actin was stained with rhodamine-phalloidin. Bar, 10 µm.

ture with astrocytes, was performed by confocal microscopy (fig. 2b). Cultured RBECs clearly expressed occludin in a continuous cell-to-cell contact. The distribution of ZO-1 in RBECs appeared as continuous lines at the cell borders. Since actin filaments also play an important role in the organization of TJs, actin was stained with rhodamine-phalloidin. Actin filaments were predominantly found at the circumference of endothelial cells. In contrast, cultures of HUVECs, which are endothelial cells of non-cerebral origin, displayed lower levels and a diffuse localization of occludin, ZO-1 and F-actin, suggesting a low degree of junctional tightness (fig. 2c).

The characterization of the in vitro BBB model was completed by measuring electrical resistance. RBECs in monoculture and coculture with astrocytes displayed TEER values increasing daily until 13 days after confluence without significant differences between the two systems. Of note is that, as shown in figure 3a, cocultures conserved high TEER values until 25 days, while RBEC monolayers (in monoculture) showed a significant decrease (fig. 3). Occludin expression was also studied as a function of culture time by Western blotting; it showed a decrease of expression after 28 days in both cases, but this decrease was more significant for the monolayer system (fig. 3b). Both these observations suggest a loss of integrity of the RBEC monolayer in the absence of coculture with astrocytes.

The functionality of our BBB model was confirmed by measuring the permeability coefficients of sucrose and inulin. Indeed, the very low paracellular Pe values of [^{14}C]sucrose ($1.86 \times \pm 0.18 \times 10^{-6}$cm/s) and [^{3}H]inulin ($1.38 \times \pm 0.36 \times 10^{-6}$cm/s) verified the establishment of an impermeable barrier. In addition, the statistical analysis demonstrated the reproducibility of our model in terms of TEER values and the permeability coefficients ($p<0.05$).

Nanoparticle translocation

The newly established BBB model was used to investigate the translocation and uptake of PHDCA and PEG-PHDCA nanoparticles. The characteristics of PHDCA and PEG-PHDCA nanoparticles were not significantly different in terms of size (166 and 171 nm, respectively). Both kinds

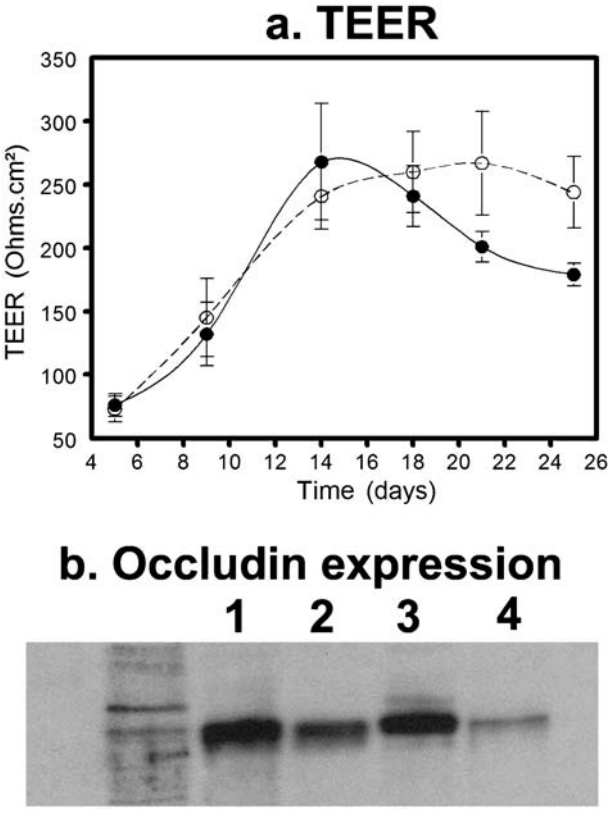

Figure 3. *a* TEER of endothelial cell monolayers in monoculture (closed circles) and coculture with astrocytes (open circles) for 3 weeks after plating onto a collagen-coated filter insert. All data are expressed as the means (n=15) ± SE. b. Western Blot analysis of occludin in RBECs in the coculture system at 13 days (lane 1), and at 28 days (lane 2); monoculture system at 13 days (lane 3) and at 28 days (lane 4).

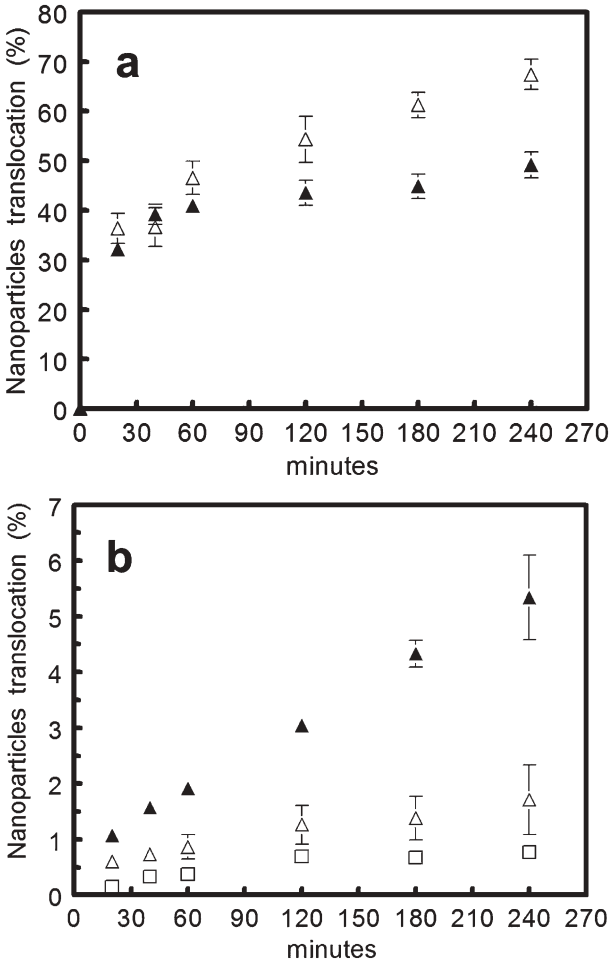

Figure 4. Translocation of radiolabeled PHDCA nanoparticles (open triangles), PEG-PHDCA nanoparticles (closed triangles) and degraded PEG-PHDCA nanoparticles (open squares) across cell-free collagen-coated filter inserts (*a*) and across RBECs after 13 days in coculture with astrocytes (*b*).

of nanoparticle freely diffused through the coated filter in the absence of cells (fig. 4a). During the incubation period, the translocation of PEG-PHDCA nanoparticles across RBECs was greater than that of PHDCA nanoparticles (fig. 4b). The same results were obtained between 13 and 17 days in monoculture, as expected (data not shown). To answer the question if the radiolabeled compounds diffused through the rat BBB model as intact nanoparticles or as their already metabolized products, we performed additional experiments with pre-degraded nanoparticles. Nanoparticle degradation products were unable to diffuse as soluble compounds through the in vitro BBB model (fig. 4b). Moreover, we confirmed the uptake of fluorescent nanoparticles by incubating nanoparticles loaded with nile red with RBECs for 1 h. The images obtained by confocal microscopy demonstrated lower uptake of PHDCA nanoparticles by RBECs (fig. 5a) in comparison with PEG-PHDCA nanoparticles (fig. 5b). The cell uptake of

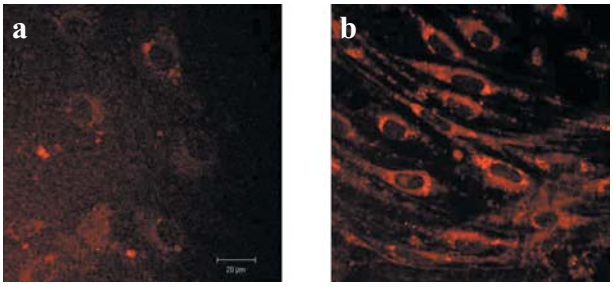

Figure 5. Confocal microscopic images of uptake of fluorescent nanoparticles composed of PHDCA (*a*) and PEG-PHDCA (*b*) by rat brain endothelial cells (13 days of culture) after 1 h of incubation.

PEG-PHDCA nanoparticles was seen as highly fluorescent punctuated patterns, preferentially located in the cytoplasm or around the nucleus.

To determine whether the passage of PEG-PHDCA nanoparticles was due to a modification in the TJs, the permeability coefficients for [^{3}H]inulin were determined in the presence and in the absence of these nanoparticles. Since the Pe values were similar in the presence and absence of nanoparticles ($1.62 \pm 0.32 \times 10^{-6}$ cm/s and $1.67 \pm 0.04 \times 10^{-6}$ cm/s, respectively), we concluded that RBEC monolayer integrity was maintained in the presence of nanoparticles. In addition, the TEER values of cocultures, during 5 h of incubation with PEG-PHDCA or PHDCA nanoparticles, were also not significantly different compared to those of cocultures without nanoparticle incubation (fig. 6). These results confirm the absence of modification of the TJs by the nanoparticles.

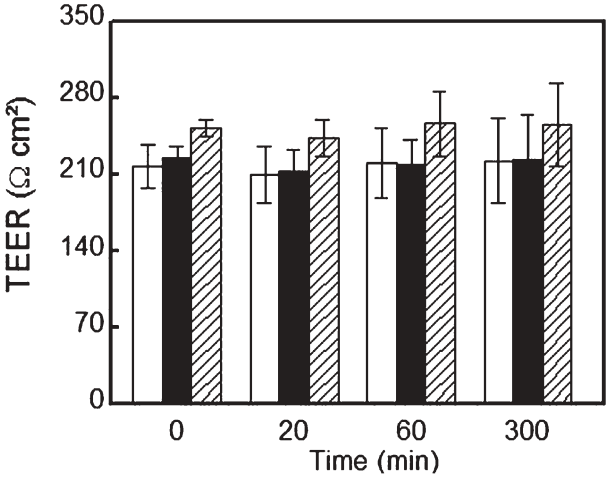

Figure 6. TEER values of cocultures (13 days of culture) without incubation of nanoparticles (open bars), with incubation of PEG-PHDCA nanoparticles (closed bars) or with incubation of PHDCA nanoparticles (hatched bars). All data are expressed as the means (n=10) ± SE.

Discussion

To assess nanoparticles transport through the BBB, we developed a syngenic in vitro BBB coculture model using RBECs and astrocytes from the same species.

The method for isolating RBECs and the use of a puromycin treatment [18] allowed high cellular density from the beginning of the culture, fast proliferation and confluence. These conditions were favorable for excluding contaminating cells which, because of their low percentage, had no opportunity to proliferate (fig. 1). The cell purity obtained in these experiments was confirmed by the high electrical resistance values (fig. 3).

One of the major problems of in vitro studies is the loss of BBB properties. However, Western blot analysis has demonstrated the expression of P-gp which is characteristic of endothelial cells in the brain tissue [26]. Another point to consider is the presence of efficient TJs between RBECs as confirmed by Western blotting and confocal microscopy (fig. 2). Confocal microscopy studies showed the presence of occludin (a transmembrane protein) and ZO-1 (a cytoplasmic protein) which are important components of TJs. The role of the N-terminal half of occludin in TJ assembly is presumed to be maintenance of the barrier function of these junctions. On the other hand, ZO-1 is bound to actin filaments and the C-terminus of occludin [27], and the structural organization of actin has been shown to influence TJ integrity [28]. The choice of these marker proteins was also justified by the fact that occludin is a well-known regulatory protein, and its presence at the BBB is correlated with increased electrical resistance across the barrier and decreased paracellular permeability [29]. Our results confirm this correlation because at 25 days of monoculture, we observed in RBECs decreases of both occludin expression and TEER values (fig. 3).

Additionally, maximum TEER values obtained after 13 days (220–300 Ωcm^2) were higher than the values reported for a coculture system of bovine brain endothelial cells and rat astrocytes at the bottom of the well, (134 Ωcm^2) [17]. At the beginning, no significant differences in TEER values were observed between the monoculture and coculture, showing that RBECs preserved BBB properties after isolation (fig. 3a). However, astrocytes were needed to maintain transendothelial electrical resistance over a period of 25 days in coculture. Several other in vitro BBB models [16, 30–32] employing brain endothelial cells after diverse subcultures have shown a dedifferentiation and loss of BBB properties. Thus, astrocytes have a remarkable influence in inducing and maintaining BBB properties, as confirmed by our results for a long period of coculture (fig. 3). Considering that RBECs could lose characteristics other than TJ functionality, which might also be important for nanoparticle translocation, we chose to build this in vitro BBB model with coculture system between RBEC and astrocytes.

The low paracellular permeability is also an indication that cultured brain endothelial cells possess junctional complexes [33]. Hence the functionality of these tight junction complexes was tested through permeability studies using radiolabeled substances such as sucrose and inulin which are impermeable markers of TJs, not taken up by the endothelial cells in vivo either by active facilitated transport. The Pes for sucrose and inulin (average molecular weight about 342 and 5000, respectively) through RBECs were in the order of $1.72 \pm 0.02 \times 10^{-6}$ cm/s and $1.28 \pm 0.01 \times 10^{-6}$ cm/s, respectively. These Pe data were similar to the values previously reported [34] in porcine brain capillary endothelial cells ($1.0 \pm 0.4 \times 10^{-6}$ cm/s for sucrose and $1.0 \pm 0.3 \times 10^{-6}$ cm/s for inulin) with TEER values of 600 Ωcm^2, four times lower, for sucrose, than the values (8.0×10^{-6} cm/s) obtained by Lundquist et al. [35] in a coculture of bovine brain endothelial cells and rat astrocytes (TEER = 800 Ωcm^2). These observations demonstrated that models with high TEER values do not necessarily show good BBB properties such as paracellular impermeability. Taken together, our data show that in the presence of rat astrocytes, RBECs formed, in our experimental conditions, a model with properties close to the in vivo situation. Other in vitro cultures of RBECs have been developed but no evaluation of the critical properties of the BBB was reported in these studies [19, 20, 36]. Thus, this model displayed characteristics and functionality consistent with the in vivo BBB and was found to be consistently reproducible enough for further investigation, as our studies on nanoparticle translocation across the BBB.

PEG-PHDCA nanoparticles showed a three fold greater crossing of the experimental BBB than PHDCA nanoparticles (4 h incubation), clearly demonstrating that the nanoparticle surface (presence of hydrophilic and flexible PEG chains) is a key parameter for intracellular uptake (fig. 4). These data correlated very well with those previously obtained in vivo after intravenous administration to the rat of PEG-PHDCA nanoparticles which concentrated more than PHDCA nanoparticles in the different brain structures [13, 24]. Thanks to the development of this rat BBB model, we have established a good in vitro/in vivo correlation and the cellular mechanisms implicated in the translocation of PEG-PHDCA and PHDCA nanoparticles through the BBB may be further investigated.

Particle surface properties are likely to play an important role in the translocation process. Both types of nanoparticle had the same size, but only nanoparticles decorated with PEG were able to cross the in vitro model of BBB. Moreover, in previous studies, the increased in vivo brain penetration of PEG-PHDCA nanoparticles was achieved without modification of BBB permeability, as determined by a sucrose assay [24]. Using the in vitro model of the

BBB developed here, we confirmed the absence of TJ modification, since TEER measurements and inulin assays showed that the increased translocation of PEG-PHDCA nanoparticles did not result from a single paracellular diffusion due to a disruption of the RBEC monolayers (fig. 6).

Nanoparticle degradation products which are constituted in major part by the hydrophilic and water-soluble poly(cyanoacrylic acid) [37, 38] did not diffuse through the cell layers (fig. 4b). The results presented here suggest that intact PEG-PHDCA nanoparticles were transported across the in vitro BBB, likely through an endocytotic process, which was also confirmed by confocal microscopy images (fig. 5).

For further study of nanoparticle translocation, an RBEC fractionation method was also developed recently [39] and showed accumulation of PEG-PHDCA nanoparticles in intracellular compartments of vesicles. On the other hand, previous studies have suggested that the mechanism for nanoparticle delivery across the BBB is most likely related to endocytosis via the low-density lipoprotein (LDL) receptor in endothelial cells that form the BBB [40]. This endocytotic uptake seems to be mediated by the adsorption of apolipoprotein B and/or E on nanoparticles from the blood. Thus, the nanoparticles could mimic lipoprotein particles and act as 'trojan horses'. In fact, Peracchia et al. [12] have observed the adsorption of apolipoprotein E onto the surface of PEG-PHDCA nanoparticles, after incubation with human citrate-stabilized plasma. Interestingly, the images of the intracellular localization of PEG-PHDCA nanoparticles (fig. 5) are similar to those of a transcellular transport as described for LDL [41].

Further experiments using this newly developed in vitro BBB model of the rat and cultures of pure RBECs are in progress to study this hypothesis of LDL-receptor-mediated endocytosis and to elucidate the pathways of nanoparticle transport.

In conclusion, this study describes an original and reproducible in vitro model of the rat BBB which presents the main morphological and functional characteristics of the BBB in vivo. Using polyalkylcyanoacrylate nanoparticles, such a model was shown to be relevant in terms of in vitro/in vivo correlations. This methodology should be a useful tool for the design of new colloidal carriers with the aim of brain drug delivery.

Acknowedgements. The authors wish to thanks Dr. I. Brigger for helpful discussions and H. Chacun, M. Appel, A. Devocelle and C. Espinasse for excellent technical assistance. E. Garcia-Garcia was supported by a scholarship from the Mexican National Council for Science and Technology (CONACYT).

1 Alyautdin R. N., Tezikov E. B., Ramge P., Kharkevich D. A., Begley D. J. and Kreuter J. (1998) Significant entry of tubocurarine into the brain of rats by adsorption to polysorbate 80-coated polybutylcyanoacrylate nanoparticles: an in situ brain perfusion study. J. Microencapsul. **15:** 67–74

2 Feng S. S., Mu L., Win K. Y. and Huang G. (2004) Nanoparticles of biodegradable polymers for clinical administration of paclitaxel. Curr. Med. Chem. **11:** 413–424

3 Kattan J., Droz J. P., Couvreur P., Marino J. P., Boutan-Laroze A., Rougier P. et al. (1992) Phase I clinical trial and pharmacokinetic evaluation of doxorubicin carried by polyisohexylcyanoacrylate nanoparticles. Invest. New Drugs **10:** 191–199

4 Kozak Y., Andrieux K., Villarroya H., Klein C., Thillaye-Goldenberg B., Naud M. C. et al. (2004) Intraocular injection of tamoxifen-loaded nanoparticles: a new treatment of experimental autoimmune uveoretinitis. Eur. J. Immunol. **34:** 3702–3712

5 Kreuter J., Alyautdin R. N., Kharkevich D. A. and Ivanov A. A. (1995) Passage of peptides through the blood-brain barrier with colloidal polymer particles (nanoparticles). Brain Res. **674:** 171–174

6 Alyautdin R. N., Petrov V. E., Langer K., Berthold A., Kharkevich D. A. and Kreuter J. (1997) Delivery of loperamide across the blood-brain barrier with polysorbate 80-coated polybutylcyanoacrylate nanoparticles. Pharm. Res. **14:** 325–328

7 Gulyaev A. E., Gelperina S. E., Skidan I. N., Antropov A. S., Kivman G. Y. and Kreuter J. (1999) Significant transport of doxorubicin into the brain with polysorbate 80-coated nanoparticles. Pharm. Res. **16:** 1564–1569

8 Olivier J. C., Fenart L., Chauvet R., Pariat C., Cecchelli R. and Couet W. (1999) Indirect evidence that drug brain targeting using polysorbate 80-coated polybutylcyanoacrylate nanoparticles is related to toxicity. Pharm. Res. **16:** 1836–1842

9 Kreuter J., Ramge P., Petrov V., Hamm S., Gelperina S. E., Engelhardt B. et al. (2003) Direct evidence that polysorbate-80-coated poly(butylcyanoacrylate) nanoparticles deliver drugs to the CNS via specific mechanisms requiring prior binding of drug to the nanoparticles. Pharm. Res. **20:** 409–416

10 Schroeder U., Sommerfeld P. and Sabel B. A. (1998) Efficacy of oral dalargin-loaded nanoparticle delivery across the blood-brain barrier. Peptides **19:** 777–780

11 Brigger I., Chaminade P., Desmaele D., Peracchia M. T., d'Angelo J., Gurny R. et al. (2000) Near infrared with principal component analysis as a novel analytical approach for nanoparticle technology. Pharm. Res. **17:** 1124–1132

12 Peracchia M. T., Harnisch S., Pinto-Alphandary H., Gulik A., Dedieu J. C., Desmaele D. et al. (1999) Visualization of in vitro protein-rejecting properties of PEGylated stealth polycyanoacrylate nanoparticles. Biomaterials **20:** 1269–1275

13 Calvo P., Gouritin B., Chacun H., Desmaele D., D'Angelo J., Noel J. P. et al. (2001) Long-circulating PEGylated polycyanoacrylate nanoparticles as new drug carrier for brain delivery. Pharm. Res. **18:** 1157–1166

14 Audus K. L. and Borchardt R. T. (1986) Characteristics of the large neutral amino acid transport system of bovine brain microvessel endothelial cell monolayers. J. Neurochem. **47:** 484–488

15 Hughes C. C. and Lantos P. L. (1989) Uptake of leucine and alanine by cultured cerebral capillary endothelial cells. Brain Res **480:** 126–132

16 Dehouck M. P., Jolliet-Riant P., Bree F., Fruchart J. C., Cecchelli R. and Tillement J. P. (1992) Drug transfer across the blood-brain barrier: correlation between in vitro and in vivo models. J. Neurochem. **58:** 1790–1797

17 Gaillard P. J., Voorwinden L. H., Nielsen J. L., Ivanov A., Atsumi R., Engman H. et al. (2001) Establishment and functional characterization of an in vitro model of the blood-brain barrier, comprising a co-culture of brain capillary endothelial cells and astrocytes. Eur. J. Pharm. Sci. **12:** 215–222

18 Perrière N., Demeuse Ph., Garcia E., Regina A., Debray M., Andreux J.-P. et al. (in press) Puromycin-based purification of rat brain capillary endothelial cell cultures; effect on the expression of blood-brain barrier specific properties. J. Neurochem.
19 Szabo C. A., Deli M. A., Ngo T. K. and Joo F. (1997) Production of pure primary rat cerebral endothelial cell culture: a comparison of different methods. Neurobiology **5:** 1–16
20 Vries H. E. de, Blom-Roosemalen M. C., Oosten M. van, Boer A. G. de, Berkel T. J. van, Breimer D. D. et al. (1996) The influence of cytokines on the integrity of the blood-brain barrier in vitro. J. Neuroimmunol. **64:** 37–43
21 Siflinger-Birnboim A., Del Vecchio P. J., Cooper J. A., Blumenstock F. A., Shepard J. M. and Malik A. B. (1987) Molecular sieving characteristics of the cultured endothelial monolayer. J. Cell Physiol. **132:** 111–117
22 Cecchelli R., Dehouck B., Descamps L., Fenart L., Buee-Scherrer V. V., Duhem C. et al. (1999) In vitro model for evaluating drug transport across the blood-brain barrier. Adv. Drug Deliv. Rev. **36:** 165–178
23 Peracchia M. T., Vauthier C., Desmaele D., Gulik A., Dedieu J. C., Demoy M. et al. (1998) Pegylated nanoparticles from a novel methoxypolyethylene glycol cyanoacrylate-hexadecyl cyanoacrylate amphiphilic copolymer. Pharm. Res. **15:** 550–556
24 Brigger I., Morizet J., Aubert G., Chacun H., Terrier-Lacombe M. J., Couvreur P. et al. (2002) Poly(ethylene glycol)-coated hexadecylcyanoacrylate nanospheres display a combined effect for brain tumor targeting. J. Pharmacol. Exp. Ther. **303:** 928–936
25 Peracchia M. T., Fattal E., Desmaele D., Besnard M., Noel J. P., Gomis J. M. et al. (1999) Stealth PEGylated polycyanoacrylate nanoparticles for intravenous administration and splenic targeting. J. Control. Release **60:** 121–128
26 Seetharaman S., Barrand M. A., Maskell L. and Scheper R. J. (1998) Multidrug resistance-related transport proteins in isolated human brain microvessels and in cells cultured from these isolates. J. Neurochem. **70:** 1151–1159
27 Furuse M., Itoh M., Hirase T., Nagafuchi A., Yonemura S. and Tsukita S. (1994) Direct association of occludin with ZO-1 and its possible involvement in the localization of occludin at tight junctions. J. Cell Biol. **127:** 1617–1626
28 Wolka A. M., Huber J. D. and Davis T. P. (2003) Pain and the blood-brain barrier: obstacles to drug delivery. Adv. Drug Deliv. Rev. **55:** 987–1006
29 Hirase T., Staddon J. M., Saitou M., Ando-Akatsuka Y., Itoh M., Furuse M. et al. (1997) Occludin as a possible determinant of tight junction permeability in endothelial cells. J. Cell Sci. **110:** 1603–1613
30 Rubin L. L., Hall D. E., Porter S., Barbu K., Cannon C., Horner H. C. et al. (1991) A cell culture model of the blood-brain barrier. J. Cell Biol. **115:** 1725–1735
31 Megard I., Garrigues A., Orlowski S., Jorajuria S., Clayette P., Ezan E. et al. (2002) A co-culture-based model of human blood-brain barrier: application to active transport of indinavir and in vivo-in vitro correlation. Brain Res. **927:** 153–167
32 MacLean A. G., Orandle M. S., MacKey J., Williams K. C., Alvarez X. and Lackner A. A. (2002) Characterization of an in vitro rhesus macaque blood-brain barrier. J. Neuroimmunol. **131:** 98–103
33 Gloor S. M., Wachtel M., Bolliger M. F., Ishihara H., Landmann R. and Frei K. (2001) Molecular and cellular permeability control at the blood-brain barrier. Brain Res. Brain Res. Rev. **36:** 258–264
34 Franke H., Galla H. and Beuckmann C. T. (2000) Primary cultures of brain microvessel endothelial cells: a valid and flexible model to study drug transport through the blood-brain barrier in vitro. Brain Res. Brain Res. Protoc. **5:** 248–256
35 Lundquist S., Renftel M., Brillault J., Fenart L., Cecchelli R. and Dehouck M. P. (2002) Prediction of drug transport through the blood-brain barrier in vivo: a comparison between two in vitro cell models. Pharm. Res. **19:** 976–981
36 Abbott N. J., Hughes C. C., Revest P. A. and Greenwood J. (1992) Development and characterisation of a rat brain capillary endothelial culture: towards an in vitro blood-brain barrier. J. Cell Sci. **103:** 23–37
37 Lenaerts V., Couvreur P., Christiaens-Leyh D., Joiris E., Roland M., Rollman B. et al. (1984) Degradation of poly(isobutyl cyanoacrylate) nanoparticles. Biomaterials **5:** 65–68
38 Vauthier C. and Couvreur P. (2002) Degradation of polycyanoacrylates. In: Handbook of Biopolymers, vol. 9, pp. 457–490, Steinbuchel A. (ed.), Wiley-VHC, Weinheim
39 Garcia-Garcia E., Andrieux K., Gil S., Kim H.R., Le Doan T., Desmaële D. et al. (in press) A methodology to study intracellular distribution of nanoparticles in brain endothelial cells. Int. J. Pharm.
40 Kreuter J., Shamenkov D., Petrov V., Ramge P., Cychutek K., Koch-Brandt C. et al. (2002) Apolipoprotein-mediated transport of nanoparticle-bound drugs across the blood-brain barrier. J. Drug Target. **10:** 317–325
41 Dehouck B., Fenart L., Dehouck M. P., Pierce A., Torpier G. and Cecchelli R. (1997) A new function for the LDL receptor: transcytosis of LDL across the blood-brain barrier. J. Cell Sci. **138:** 877–889